The electronic effects of ligands on metal-coordination geometry: a key role in the visual discrimination of dimethylaminopyridine and its application towards chemo-switch†

Weiwei Fang,[a] Cong Liu,[ab] Jiangbo Chen,[a] Zhengwei Lu,[a] Zhi-Ming Li,*[a] Xiaoling Bao[c] and Tao Tu*[ab]

Due to its special coordination ability to Cu(II)−terpyridine complexes, a simple and straightforward visual recognition of *p*-DMAP out of its analogues has been realized *via* selective metallogel collapse. In combination with the selective gel collapse and the self-healing properties of metallohydrogel 1a, its potential application towards chemo-switch is also demonstrated.

Due to their broad applications in chemistry and material sciences, functional molecular gels have drawn considerable attention.[1,2] In comparison with organogels, less-studied metallogels represent some of the most intriguing "smart" materials,[3] because the incorporation of transition metals into gelator molecules not only integrates the metal characteristics (including conductive, redox, catalytic or luminescent properties) into the gel, but also provides an additional subtle control of the molecular assembly. Among non-covalent weak interactions, metal–metal interactions constitute a main driving force leading to metallogel formation.[3a] Therefore, structural modification by suitable guest molecules might handicap or assist these metal interactions to allow a control over metallogels, indicating metallogels as a conceptually new platform for visual molecular discrimination.[1d] With this in mind, our group firstly realized an unprecedented visual discrimination of enantiomers of chiral phosphines *via* metallogels based on platinum pincer complexes.[4]

Subsequently, our research was extended to metallo-hydrogels derived from terpyridine metal complexes to explore their potential applications in visual recognition.[5] It was suggested that the balance

of metal–metal interaction, π−π stacking and hydrogen bonding between the gelator and water molecules exhibits a crucial impact on the gel. In combination with the special coordination ability of Cu(II) ions to the N-ligands using our metal–ligand interaction blocking strategy, the addition of bulky terpyridines or bidentate ligands like bipyridines into metallo-hydrogel **1a** resulted in gel collapse after chloride substitution and ligand chelation (Fig. 1a).[5b,c] In contrast to a plenty of examples of chemical triggering organogels, exploration of less-studied intriguing metallogels towards molecular switches still constitutes a challenging task.[6] Accordingly, the feasibility of these terpyridine metallogels towards photo- and chemo-switches has also been demonstrated.[5a,b] Besides the multidentate ligands, mono-dentate pyridine (Py) and its derivatives are considered as a class of the most important ligands.[7] However, in general, the less-hindered mono-dentate ligands like Py are considered as an unlikely option to control the gel properties. Following our recent research interest in exploring novel pincer metal complexes towards sensing, catalysis and materials science,[4,5,8,9] herein, we would like to probe the responsive behaviors and feasibility of metallo-hydrogels based on Cu(II) pincer complexes (**1–5**) with additional mono-dentate pyridine derivatives (Fig. 1b). Along with determining the intrinsic correlation between the metal coordination
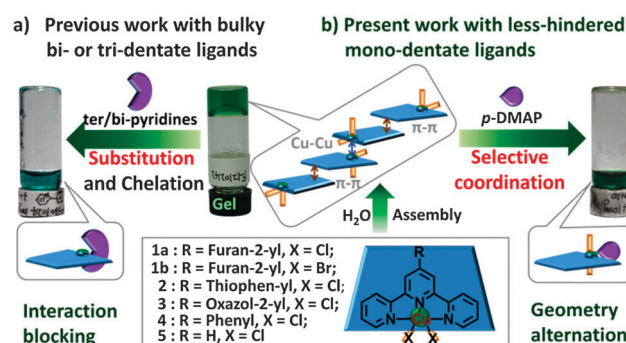
[a] *Department of Chemistry, Fudan University, 220 Handan Road, Shanghai, 200433, China. E-mail: taotu@fudan.edu.cn*

[b] *State Key Laboratory of Organometallic Chemistry, Shanghai Institute of Organic Chemistry, Chinese Academy of Sciences, Shanghai, 200032, China*

[c] *Institute of Quality Inspection of Food and Cosmetics, Shanghai Institute of Quality Inspection and Technical Research, 381 Cangwu Road, Shanghai, 200233, China*

† Electronic supplementary information (ESI) available: [1H] NMR, [13C] NMR and ESI-MS spectra, the single crystal study, DFT theoretical calculations, SEM and TEM morphologies. CCDC 1045806–1045809. For ESI and crystallographic data in CIF or other electronic format see DOI: 10.1039/c5cc00196j

Fig. 1 Control over metallo-hydrogel collapse *via* different strategies: (a) halide substitution with a bulky multi-dentate ligand and ligand chelation; (b) selective coordination with a mono-dentate ligand.

geometry and molecular assembly, their potential application towards chemo-switch was also demonstrated.

As we previously reported, terpyridine complex **1a** readily gelates water even without heating and cooling operation. The critical gelator concentration is 0.25 wt%, therefore, complex **1a** is regarded as a super hydrogelator.[5c] In consideration of its coordination propensity to Cu(II) ions, Py was selected to investigate its impact on high thermo-stable metallo-hydrogel **1a** (1 wt%, the corresponding gel–sol phase-transition temperature is 74 °C). After the addition of 1 equiv. of Py to metallogel **1a** (1 wt%), no obvious collapse was observed. Upon increasing the amount of Py to 12 equiv., gel collapse was finally realized after the identical operations. A variety of pyridine derivatives were then screened. However, only the addition of 4-dimethylaminopyridine (*p*-DMAP) led to instant gel collapse without heating; other pyridine derivatives failed to achieve the goal (Fig. 2c). Among pincer complexes **1b**–**5** with different substituents at the 4′-position, only complexes **1b** and **4** gelated water to form stable hydrogels (1 wt%, Fig. 2a). However, regardless of the phase, all selected samples rapidly transformed into clear green solutions after the addition of 1 equiv. of *p*-DMAP. Delightedly, blue–green rectangular single crystals **6a**–**8**, which are suitable for X-ray analysis, were gradually grown from the corresponding solutions (Fig. S7–S12, ESI†).

As shown in Fig. 2b, the Cu(II) center of complex **6a** adopted a six-coordination geometry, in which the Py-ring was almost perpendicular to the terpyridine plane. The bond distance of Cu–N_DMAP was slightly longer than that of the central Cu–N_tpy (1.97 Å *vs.* 1.93 Å); and two side Cu–N_tpy bonds were equal (2.03 Å). The Cl ligands occupied the axial positions, however, the difference between these two Cu–Cl bonds was significant: one was 2.68 Å and the other was 3.23 Å. The elongated octahedral geometry of complex **6a** clearly indicated that there is a strong Jahn–Teller effect,[10] which would significantly enhance the complex stability. Although there were obvious π–π interactions (between the furan ring and one of the arm of the Py-ring of the second molecule, 4.01 Å), no evident Cu–Cu interactions were found, due to the special elongated octahedral geometry (Fig. S8, ESI†). Distorted octahedral geometries, similar bond lengths and interactions were also found in the crystal structures of complexes **7** and **8** (Fig. S9–S12, ESI†). With the data obtained so far, we may presume that *p*-DMAP was inclined to coordinate with the Cu(II) center resulting in six-coordination adducts with elongated octahedral geometry, which efficiently interrupted the possible Cu–Cu interaction,[5b,c] leading to gel collapse. Additionally, UV-vis studies also supported the selective coordination ability of *p*-DMAP towards pincer Cu(II) complexes (Fig. S16–S18, ESI†).

Taking into account the dimethylamino group (Me₂N) as a strong electron-donating group, which readily enhances the electron density of the *para*-N atom and its coordination ability, a series of pyridine derivatives with *para*-substituents, such as isonicotinonitrile (*p*-CNP), 4-diethylaminopyridine (*p*-DEAP), 4-(4-morpholinyl)-pyridine (*p*-MPP), 4-methoxy pyridine (*p*-MOP) and 4-methylpyridine (4-MeP), as well as two *p*-DMAP positional isomers (*o*-DMAP or *m*-DMAP), were selected to test their gel collapse ability (Fig. 2d and S6, ESI†). Upon the addition of 1 equiv. of *p*-DEAP on the top of gel **1a**, instant gel collapsing was also observed. However, other pyridines all failed to collapse the gel. The B3LYP density functional theory (DFT) calculations at the 6-31G(d) level were carried out using Gaussian 09 package to probe the mechanism, in which the nucleophilicity of tetracyanoethylene (TCE) was used as the reference.[12–14] The HOMO, LUMO energies, the global nucleophilicity indices (*N*) and charges at the N atom of the selected pyridines were compiled in Table 1. Unlike *p*-CNP, Py, *p*-MeP and *p*-MOP (entries 1–4, Table 1), *p*-DMAP and *p*-DEAP were assigned as the strong nucleophiles (entries 6 and 9, Table 1). Due to the electron-withdrawing properties of oxygen atoms, the *N* value of *p*-MPP was inferior to those of *p*-DMAP and *p*-DEAP (Table 1).

In order to explain the gel collapse with 12 equiv. of Py, we aimed to synthesize complex **9** (Scheme 1), in which one Cl ligand was substituted by Py. However, when 1 equiv. of silver triflate (AgOTf) and 2 equiv. of Py in methanol at room temperature reacted with complex **1a**, instead of complex **9**, distorted square planar
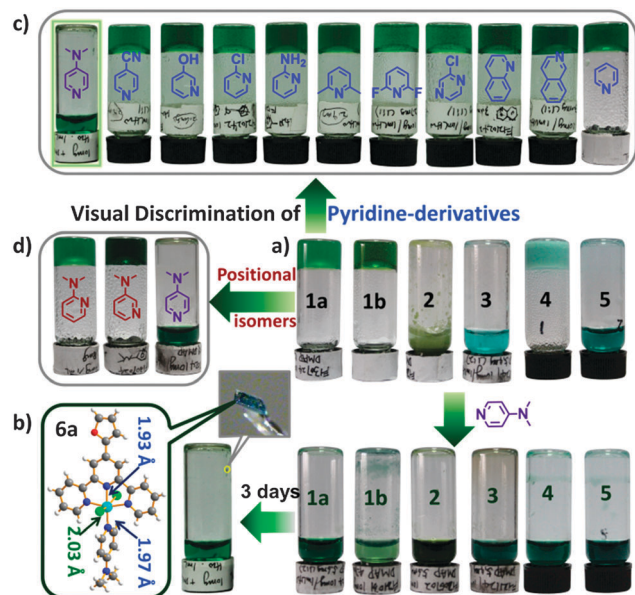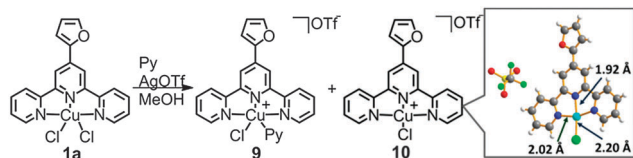

Fig. 2 (a) Gelation test with Cu–pincer complexes **1–5** and additional *p*-DMAP; (b) a crystal growth of adduct **6a** *in situ* from the collapsed sol [**1a** + *p*-DMAP] and the relative molecular structure of complex **6a**; selective metallo-hydrogel **1a** (1 wt%) collapse with (c) additional pyridine derivatives or (d) DMAP positional isomers.

Table 1 The calculated global properties of selected nucleophiles[a]

Entry	R-Py	HOMO	LUMO	N	Charge at N atom (e)
1	*p*-CNP	0.2797	−0.0763	1.51	−0.432
2	Py	0.2526	−0.0225	2.25	−0.452
3	*p*-MeP	0.2496	−0.0183	2.33	−0.458
4	*p*-MOP	0.2450	−0.0076	2.46	−0.476
5	*p*-MPP	0.2156	−0.0044	3.26	−0.481
6	*p*-DMAP	0.2055	0.0059	**3.54**	−0.490
7	*o*-DMAP	0.1939	−0.0070	3.85	−0.519
8	*m*-DMAP	0.1934	−0.0075	3.87	−0.438
9	*p*-DEAP	0.2025	0.0049	3.62	−0.493
10	Piperidine	0.2090	0.0825	3.44	−0.691
11	*p*-DMAP·TFA	0.2530	−0.0287	**2.23**	−0.460

[a] HOMO, LUMO in au; global nucleophilicity (*N*), and values in eV.

Scheme 1 Synthesis of planar pincer complex **10** and its crystal structure.
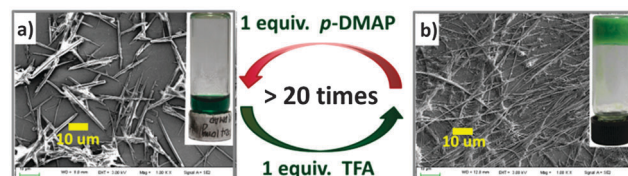

Fig. 3 Gel collapse and reformation processes by adding *p*-DMAP and TFA, subsequently. SEM images of: (a) collapsed sol [**1a** + *p*-DMAP/TFA + *p*-DMAP] and (b) reformed gel [**1a** + *p*-DMAP/TFA].

four-coordination Cu(II) complex **10** was obtained, which was confirmed by the X-ray crystal structure obtained by direct evaporation of complex **10** in methanol. In comparison with complex **6a**, similar Cu–N$_{tpy}$ bond lengths (1.92 Å and 2.02 Å) were observed. However, the length of Cu–Cl in the structure of complex **10** was only 2.20 Å. Obvious π–π and Cu–Cu interactions between the molecules were found, which were much shorter than what were observed in the crystal of complex **1a** (3.71 Å *vs.* 4.10 Å, Fig. S13 and 14, ESI†).[5c] Due to the efficient molecular packing,[11] compound **10** hardly gelated any selected organic solvents and water.

Using natural bond orbital (NBO) analysis,[15] the charges at the N atom of *p*-DMAP and *p*-DEAP were also calculated, which were much higher than what were observed with other pyridine derivatives. In the cases of *o*- and *m*-DMAP, the global nucleophilicity *N* values were almost equal to each other (entries 7 and 8, Table 1). Especially, the charge at the N atom of *o*-DMAP was the richest among three positional isomers (−0.519 *vs.* −0.438 and −0.490, Table 1), however, *o*-DMAP was ineffective in collapsing gel **1a**. After detailed energy optimization of three possible isomers **6a–c** formed by complex **1a** and *p*-, *m*- or *o*-DMAPs at M06/6-31+G(d) with the SDD (on Cu) level,[16] respectively, adduct **6a** was calculated as the most stable isomer (Table S26, Fig. S15, ESI†). Although, the free energy of isomer **6c** was little lower than that of **6a** in 0.6 kcal mol^{-1}, the distance of N$_{DMAP}$–Cu (3.70 Å) as well as steric hindrance between the –NMe$_2$ group and the terpyridine skeleton suggested that complex **6c** was thermodynamically unstable.

Piperidine has a similar nucleophilicity (3.44 *vs.* 3.54, Table 1) and a higher pK_a value (11.21 *vs.* 9.70, Table S25, ESI†) than those of *p*-DMAP. However, the addition of 1 equiv. of piperidine failed to collapse metallogel **1a**, which may reveal that the coordination ability of the guest molecule plays a predominant role in the gel formation/collapse rather than its pK_a value. With this clue in mind, alternation of the electron density of the guest is expected to provide a control over gel collapse and reformation. Therefore, trifluoroacetic acid (TFA) was chosen for this purpose. As we expected, gel reformation of the collapsed sol [**1a** + *p*-DMAP] (1 wt%) was observed upon addition of 1 equiv. of TFA (Fig. 3). Using ^{1}H NMR spectroscopy, upon addition of 1 equiv. of TFA into a CDCl$_3$ solution of *p*-DMAP, the proton signals related to the Me$_2$N group were obviously downfield shifted (*e.g.* –CH_3 shifted from 2.99 to 3.22 ppm), while no obvious shift was observed for the α-protons of the pyridine ring (Fig. S29, ESI†). With additional TFA, no change was observed, and it clearly indicated that TFA only selectively protonated the Me$_2$N group, which was quite different to the previous reports.[17] After protonation, the *N* value was decreased

from 3.54 to 2.23 (entry 11, Table 1), which was even inferior to that of Py. Hence, *p*-DMAP·TFA readily dissociated from complex **6a**. To our delight, we successfully realized the reversible gel-to-sol phase transition more than twenty times. In consideration of the gel-reformation of the sol [**1a** + 100 equiv. *p*-DMAP] being still observed upon addition of 100 equiv. of TFA, this new metallo-hydrogel chemo-switch system should be highly fatigue-resistant.[1d,5a] Furthermore, the gel re-formation process was further investigated by SEM and TEM. Unlike the nanoparticle morphology observed with metallo-hydrogel **1a**,[5c] dense long nanofiber networks were observed in all re-formed metallo-hydrogels [**1a** + *p*-DMAP/TFA] (Fig. 3b, ESI†). In contrast, bulky rectangular crystalline rods were found in all collapsed sols [**1a** + *p*-DMAP/TFA + *p*-DMAP] (Fig. 3a, ESI†).

In summary, a simple, convenient and straightforward visual discrimination of *p*-DMAP out of its positional isomers and other analogues has been realized by using metallo-hydrogels based on pincer terpyridine Cu(II) complexes *via* selective gel collapse. With the assistance of single crystal analysis, theoretical calculations, NMR, SEM and TEM morphology studies, the electron properties of pyridine derivatives play a crucial role in the highly selective coordination to the Cu(II) center. The resulted six-coordination adduct with octahedral geometry apparently blocks the Cu–Cu interaction leading to gel collapse. In combination with the selective coordination ability of mono-dentate pyridine derivatives and the self-healing ability of metallo-hydrogel **1a**, the reversible gel-to-sol phase transition has been achieved more than 20 times by the addition of *p*-DMAP and TFA, subsequently. The inspiring outcome highlights their feasibility towards chemo-switch.

Notes and references

1 (*a*) D. K. Kumar and J. W. Steed, *Chem. Soc. Rev.*, 2014, **43**, 2080; (*b*) L. Zhang, L. Qin, X. Wang, H. Cao and M. Liu, *Adv. Mater.*, 2014, **26**, 6959; (*c*) T. Tu, W. Fang and Z. Sun, *Adv. Mater.*, 2013, **25**, 5304; (*d*) J. W. Steed, *Chem. Soc. Rev.*, 2010, **39**, 3686; (*e*) N. M. Sangeetha and U. Maitra, *Chem. Soc. Rev.*, 2005, **34**, 821.
2 (*a*) X. Yu, L. Chen, M. Zhang and T. Yi, *Chem. Soc. Rev.*, 2014, **43**, 5346; (*b*) P. Duan, H. Cao, L. Zhang and M. Liu, *Soft Matter*, 2014,

10, 5428; (c) L. A. Estroff and A. D. Hamilton, *Chem. Rev.*, 2004, **104**, 1201.

3 (a) A. Y.-Y. Tam and V. W.-W. Yam, *Chem. Soc. Rev.*, 2013, **42**, 1540; (b) J. H. Jung, J. H. Lee, J. R. Silverman and G. John, *Chem. Soc. Rev.*, 2013, **42**, 924; (c) J. Zhang and C.-Y. Su, *Coord. Chem. Rev.*, 2013, **257**, 1373; (d) M.-O. M. Piepenbrock, G. O. Lloyd, N. Clarke and J. W. Steed, *Chem. Rev.*, 2010, **110**, 1960; (e) X. Chen, Z. Huang, S.-Y. Chen, K. Li, X.-Q. Yu and L. Pu, *J. Am. Chem. Soc.*, 2010, **132**, 7297; (f) S. Zhang, S. Yang, J. Lan, Y. Tang, Y. Xue and J. You, *J. Am. Chem. Soc.*, 2009, **131**, 1689.

4 T. Tu, W. Fang, X. Bao, X. Li and K. H. Dötz, *Angew. Chem., Int. Ed.*, 2011, **50**, 6601.

5 (a) W. Fang, C. Liu, Z. Lu, Z. Sun and T. Tu, *Chem. Commun.*, 2014, **50**, 10118; (b) W. Fang, X. Liu, Z. Lu and T. Tu, *Chem. Commun.*, 2014, **50**, 3313; (c) W. Fang, Z. Sun and T. Tu, *J. Phys. Chem. C*, 2013, **117**, 25185.

6 (a) Z. Sun, Z. Li, Y. He, R. Shen, L. Deng, M. Yang, Y. Liang and Y. Zhang, *J. Am. Chem. Soc.*, 2013, **135**, 13379; (b) G. O. Lloyd and J. W. Steed, *Nat. Chem.*, 2009, **1**, 437.

7 (a) M. Schlosser and F. Mongin, *Chem. Soc. Rev.*, 2007, **36**, 1161; (b) E. F. V. Scriven, *Chem. Soc. Rev.*, 1983, **12**, 129.

8 (a) M. Xu, X. Li, Z. Sun and T. Tu, *Chem. Commun.*, 2013, **49**, 11539; (b) T. Tu, H. Mao, C. Herbert, M. Xu and K. H. Dötz, *Chem. Commun.*, 2010, **46**, 7796; (c) T. Tu, X. Feng, Z. Wang and X. Liu, *Dalton Trans.*, 2010, **39**, 10598; (d) T. Tu, J. Malineni, X. Bao and K. H. Dötz, *Adv. Synth. Catal.*, 2009, **351**, 1029; (e) T. Tu, J. Malineni and K. H. Dötz, *Adv. Synth. Catal.*, 2008, **350**, 1791; (f) Z. Wang, X. Feng, W. Fang and T. Tu, *Synlett*, 2011, 951.

9 (a) T. Tu, X. Bao, W. Assenmacher, H. Peterlik, J. Daniels and K. H. Dötz, *Chem. – Eur. J.*, 2009, **15**, 1853; (b) T. Tu, W. Assenmacher, H. Peterlik, G. Schnakenburg and K. H. Dötz, *Angew. Chem., Int. Ed.*, 2008, **47**, 7127; (c) T. Tu, W. Assenmacher, H. Peterlik, R. Weisbarth, M. Nieger and K. H. Dötz, *Angew. Chem., Int. Ed.*, 2007, **46**, 6368.

10 (a) D. Reinen, M. Atanasov, P. Köhler and D. Babel, *Coord. Chem. Rev.*, 2010, **254**, 2703; (b) E. C. Constable, C. E. Housecroft, J. R. Price and J. A. Zampese, *CrystEngComm*, 2010, **12**, 3163; (c) B. Murphy and B. Hathaway, *Coord. Chem. Rev.*, 2003, **243**, 237.

11 K. Liu, L. Meng, S. Mo, M. Zhang, Y. Mao, X. Cao, C. Huang and T. Yi, *J. Mater. Chem. C*, 2013, **1**, 1753.

12 L. R. Domingo, M. J. Aurell, P. Pérez and R. Contreras, *Tetrahedron*, 2002, **58**, 4417.

13 M. J. Frisch, *et al. Gaussian 09, Revision A.02*, 2009.

14 (a) L. R. Domingo, E. Chamorro and P. Pérez, *J. Org. Chem.*, 2008, **73**, 4615; (b) R. G. Parr, L. V. Szentpály and S. Liu, *J. Am. Chem. Soc.*, 1999, **121**, 1922; (c) R. G. Parr and P. K. Chattaraj, *J. Am. Chem. Soc.*, 1991, **113**, 1854; (d) R. G. Pearson, *J. Chem. Educ.*, 1987, **64**, 561.

15 (a) A. E. Reed, L. A. Curtiss and F. Weinhold, *Chem. Rev.*, 1988, **88**, 899; (b) A. E. Reed, R. B. Weinstock and F. Weinhold, *J. Chem. Phys.*, 1985, **83**, 735.

16 (a) Y. Zhao and D. G. Truhlar, *Acc. Chem. Res.*, 2008, **41**, 157; (b) T. H. Dunning Jr. and P. J. Hay, in *Modern Theoretical Chemistry*, ed. H. F. Schaefer III, Plenum, New York, 1977, vol. 3, pp. 1–28.

17 J. E. Beves, V. Blanco, B. A. Blight, R. Carrillo, D. M. D'Souza, D. Howgego, D. A. Leigh, A. M. Z. Slawin and M. D. Symes, *J. Am. Chem. Soc.*, 2014, **136**, 2094.